An Interference of High Frequency Series Resonant Inverter in Domestic Induction Heater Estimation in Emission Control Using FEM

Agamani Chakraborty[a], Debabrata Royi[b], Pradip Kumar Sadhu[c], Ankur Ganguly[d], Atanu Banerjee[c,]

[a]*Asansol Engineering College,Asansol-713305, West Bengal,India*
[b]*Batanagar Institute of Engineering, Management & Science, Kolkata – 700141, West Bengal, India*
[c]*Indian School of Mines, Dhanbad – 826004, Jharkhand, India*
[d]*Batanagar Institute of Engineering, Management & Science, Kolkata – 700141, West Bengal, India*

Abstract

This work describes a new technology to calculate the magnetic field emission of a High Frequency Series Resonant Inverter in a domestic induction heater by means of computational simulations. The calculation is performed assuming normal operation conditions required to measure the magnetic field by means of a triple loop antenna. This triple loop antenna, also known as a van Veen & Bergervoet antenna, is generally employed to test compliance with emission regulations in the frequency range of band A and band B i.e. 5-55 kHz.

Keywords: FEM, full bridge resonant inverters, induction heater, high frequency

1. Introduction

In domestic applications [1] electric apparatus must comply with various regulations in order to guarantee harmless operation conditions for the user and other electrical machines. Among others, emission [2] disturbance regulations have been defined to minimize magnetic interferences in order to protect other electrical devices against external electromagnetic fields [3]. In that case, the mandatory regulation is adapted from the international recommendations termed CISPR-16 (from Comité International Spécial des Perturbations Radioélectriques). These documents define the procedure to measure interference disturbances in medium frequencies by using Large-Loop Antennas (LLAs). LLAs were proposed by van Veen & Bergervoet in order to determine the dipolar magnetic contribution to the electromagnetic field of a medium size source located in the middle. LLAs were subsequently studied by other researcher to prove their usefulness in determining the emitted interference of a wide variety of devices. The probe planned in the recommendation consists of three LLAs placed in perpendicular directions called LLAX, LLAY and LLAZ, respectively, as shown in Fig. 1, where the subscript denotes the normal vector of the plane defined by the loop antenna. It should be noted that the magnetic field arises from closed loop current densities in the devices; consequently, the projection of the current densities in a plane is associated with the dipolar moment directed along the normal vector to the plane. As a result, each large loop antenna detects the dipolar moment component directed along the normal vector to the LLA plane. Thus LLAX and LLAY antennas, the so called vertical antennas, measure the vertical current loops densities, whereas LLAZ, called the horizontal antenna, determines the effect arising from horizontal current densities. In this research work, a procedure to simulate and predict the emission levels arising from a high frequency series resonant inverter in a domestic induction heater is proposed. These devices consist of three or four burners on which is placed a ferromagnetic type pot, which is heated up by the variable magnetic field generated by the inductor system situated below. As a rule, a high frequency series resonant inverter provides a medium frequency current, ranging between 5 and 100 kHz to the induction-heated system to the inductor system, in order to deliver a power of 2 kW into the pot. In this paper the main discussion is on the mathematical calculation of the emission of a high frequency series resonant inverter [4] used in a domestic induction heater in order to estimate compliance with respect to the limits specified in the standard EN 50011.

---

*Corresponding author
Email address:* agamani_chakraborty@yahoo.co.in (Agamani Chakraborty)
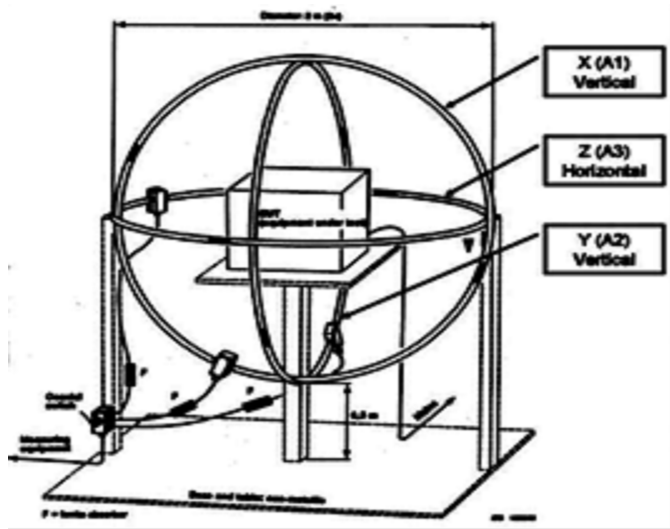
Figure 1: Triple loop antenna designed to evaluate the magnetic disturbance of the equipment under test (CISPR16-1-3)

2. Characterization of the Induction Heating System

The high frequency resonant inverter lies at the heart of induction heating [5, 6] systems. This system may operate efficiently under the condition of power factor close to unity. The main requirements for the high frequency resonant inverter are switching in the high-frequency range [7], high efficiency, wide power range and reliability.

Induction heaters are usually designed to operate with a vessel made from a specific material, primarily ferromagnetic stainless steel. Therefore desired characteristics for the inverter are: no reactive components other than the heating coil and the non-smooth filter inductor, no input or matching transformers, 50 duty ratio that simplifies the control and gate circuits, zero current switching (ZCS) and/or zero voltage switching (ZVS), clamped switch voltage and/or current. One uncontrolled voltage source is used. Induction heating power [8] supplies are frequency changers that convert the available utility line frequency power to single phase power at a frequency appropriate for the induction heating process. They are often referred to as converters, inverters or oscillators. But they are generally a combination of the above mentioned circuits. The converter section of the power supply converts the line frequency alternating current to direct current, and the inverter or oscillator portion changes the direct current to single phase alternating current of the required frequency for induction heating purposes. Different types of power supply and models are available to meet the heating requirements of a nearly endless variety of induction heating applications. The frequency, power level and other parameters like coil voltage, coil current and power factor are decided by the specific application. Fig. 2 shows common applications of induction-heated systems. Fig. 3 illustrates this same relationship for induction heating prior to metal forming operations.
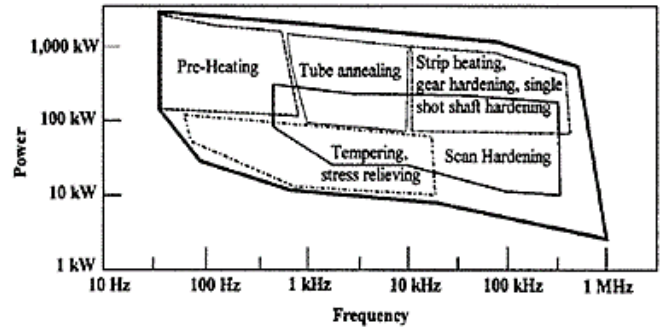

Figure 2: Power-frequency diagram for typical induction heat treating applications
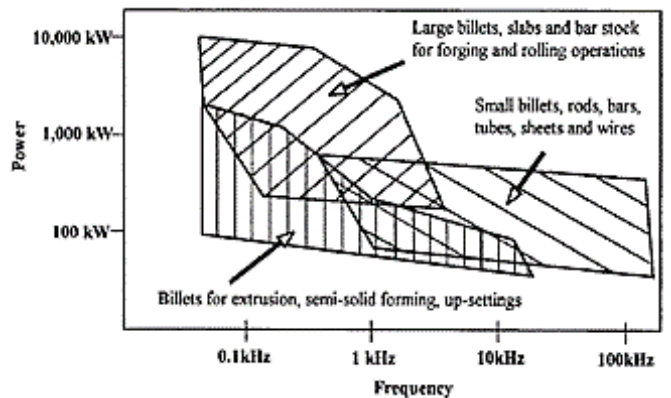

Figure 3: Power-frequency diagram for typical induction heating prior to metal forming

The selection of frequency is a key parameter in induction heating treatment, because it is the primary control over the depth of current penetration. Moreover, the frequency also plays an important role in the design of induction heating power supplies, because the power devices must be rated for operation at a specific frequency. The power circuit must ensure that these components are operated with adequate margin to yield high reliability at this frequency. Very early power supplies used high power vacuum tubes in an oscillator circuit to generate the radio frequency that was used for induction heating. Modern induction heating power supplies utilize power semiconductors such as SCR (Silicon-Controlled Rectifier), GTO (Gate turn-off thyristor), BJT (Bipolar Junction Transistor), MOSFET (metal–oxide–semiconductor field-effect transistor), IGBT (insulated-gate bipolar transistor), MCT (MOS-controlled thyristor) etc. to switch the direction of current flow from a direct current source to produce alternating current at a frequency suitable for induction heating. Fig. 4 shows graphic depictions of the various combinations of power and frequency ranges that are covered by power supplies using thyristors, transistors or vacuum tubes. There are obviously large areas of overlap where more than one type of power supply can be used.
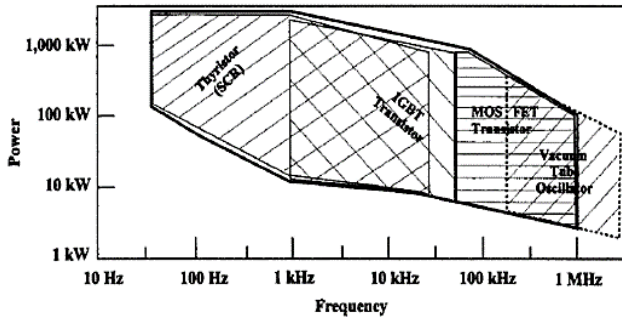
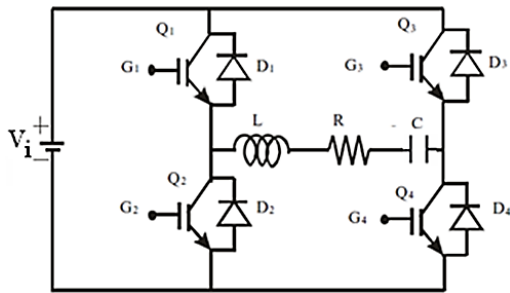Figure 4: Power semiconductors used for induction heating

Figure 6: FEA-tool based simulations results of a domestic induction heater with pot acting as the system load

Figure 5: Full bridge series resonant inverter

In the proposed topology Bm in air is low. Thus, to generate sufficient eddy current loss, the frequency f is required to be as high as possible. Accordingly, the frequency should be in the radio frequency range to keep the product ($f(B_m)$) high. In view of saving electrical energy in various home appliances, it is better to implement the high frequency inverter topology. Full bridge circuit is normally used for higher output power. Basic circuit is shown in Fig. 5. Four solid state switches are used and two switches are triggered simultaneously. Anti-parallel diodes are connected with the switch that allows the current to flow when the main switch is turned OFF.

The circuit is on when switches $Q1$ and $Q4$ are triggered simultaneously. The current flows for a half cycle of the resonant frequency and becomes zero when both switches $Q1$ and $Q4$ are turned off. When $Q1$ and $Q4$ stop conducting and switches $Q2$ and $Q3$ are not yet turned ON, the current through the load reverses and is now carried by $D1$ and $D4$, the anti-parallel diodes which are connected with the respective switches. The voltage drops across diodes appear as a reverse bias for switches $Q1$ and $Q4$. If the duration of the reverse bias is more than the turn-off time, then switches $Q1$ and $Q4$ get commutated naturally and therefore, a commutation circuit is not required. This method of commutation is called load commutation and used in high frequency inverters for induction heating. Fig. 6 shows the FEA-tool based simulations results of a domestic induction heater with pot acting as the system load.

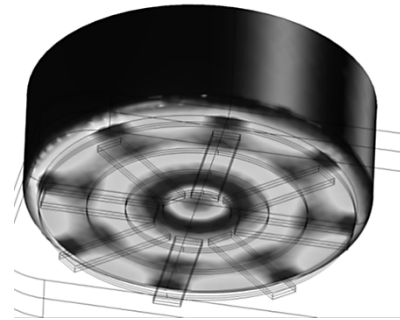The high frequency series resonant inverter in a domes-

tic heater load system can be electrically modelled [9] as an RLC-series equivalent. The frequency dependent equivalent impedance $Z(f)$ of the inductor-pot system is extracted from the FEA (Finite Element [10] Analysis)-tool model depicted in Fig. 6, as well as the electromagnetic fields of the induction system, therefore, the induced voltage VLLA (Voltage of Large-Loop Antennas), $X(f)$, VLLA, $Y(f)$, and VLLA, $Z(f)$ in each LLA are synchronously calculated. The high frequency series resonant inverter employed in the induction system in the domestic induction heater was modelled with the pot over the cooking surface at a distance of 2—6 mm above the inductor. The pot is misaligned with respect to the inductor 25 mm along the normal direction of the LLAX, therefore, large signal levels were obtained for the LLAY and the LLAZ. It should be noted that that the largest emission levels are associated with the LLAZ for a centered pot, because the majority of the field sources are current loop densities parallel to the plane of this antenna. The coil is modelled as an external current distribution, Je, whereas the pot and the shielding (usually an aluminum sheet which protects the power electronics converter placed under the inductor-pot system) are included, assuming the approach of the impedance boundary condition which is suitable for good conductor materials. Finally, the flux concentrator added to increase the coupling between the magnetic fields of the coil and the pot are modelled with bars of high permeability material. It should be noted that the half-bridge inverter working in normal mode acts as a voltage source with output of $v_0(t)$. This $v_0(t)$ is a rectangular pulse train with period equal to the inverse of the switching frequency (fsw) and amplitude values equal to $0V$ or bus voltage, V_{bus}, the latter being equal to the voltage taken from the network and subsequently rectified. Thus, the Fourier series of the inverter output voltage, $v_0(t)$, is given by:

$$v_0(t) = V_{bus} \sum V_{rect,n} e^{j2\pi f st} \tag{1}$$

Where V_{bus} is equal to $745 \sqrt{2 |\sin(100\pi t)|}$ because it is the rectified voltage from the mains, and $V_{rect,n}$ corresponds with the nth harmonic of the decomposition of a rectangular pulsation sequence, therefore:
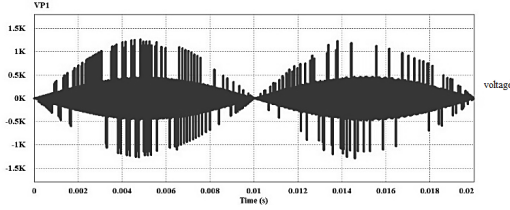
Figure 7: Harmonic content of the output of High Frequency Series resonant inverter voltage simulation values symbolized
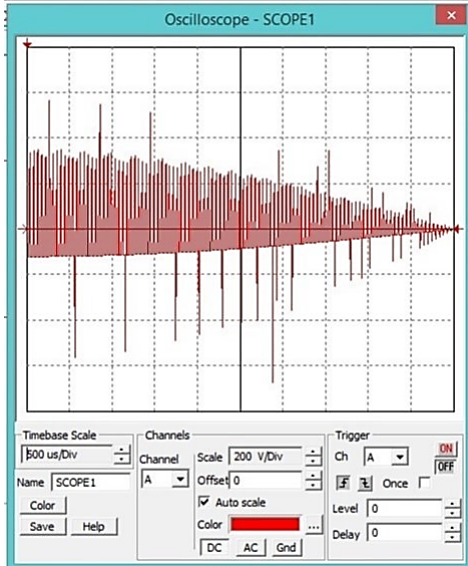

Figure 8: Harmonic content of the output of High Frequency Series resonant inverter voltage simulation values symbolized in real time experimental setup

$$v_{net,n} = 1/j2\pi n \quad n = \text{odd}$$
$$= 1/2 \qquad n = 0 \qquad (2)$$
$$= 0, \qquad n = \text{even}$$

An assessment was made between the theoretical values and the voltage amplitude obtained from experimental work [11] for per capita harmonic of the inverter output voltage. The results of the experiment are depicted in Fig. 7 and Fig. 8 which show good settlement between them. The current carried by the inductor, $i_0(t)$, can also be expressed by the Fourier series expansion, where each harmonic of the current, $i_{0,n}$, is determined by the ratio between the corresponding harmonic of the output voltage, $V_{0,n}$, and the impedance of the resonant tank, $Z_{0,n}$, which is equal to:

$$Z_{0,n}(nfs) = (nf_2) + \frac{1}{j2nf_sC_r} \qquad (3)$$

Where: $Z_{0,n}$ is the nth harmonic of the equivalent impedance of the inductor-pot system and c_r is the value of the resonant capacitor connected in series with the inductor.

3. Mathematical Analysis

Of the many mathematical calculations performed, only one specific analysis is presented here [12]. Emission control with 2500 W domestic induction heater is achieved. Finite Element Analysis (FEA) is employed to confirm whether 2500 W input power is obtained in a domestic induction-heated system. After performing FEA it is found to obtain an input power of 2463.92 W i.e almost 2500 W. A coil used in an induction heater with diameter $D = 0.02$ m, length $L = 0.05$ m and thermal conductivity $k = 50$ W/(m°C) is exposed to ambient air at $T_\alpha = 500°$C with a heat transfer coefficient $\beta = 100$ W/(m^2,°C). The left end of the coil is maintained at temperature $T_0 = 1000°$C and other end is insulated. The objective is to determine the temperature distribution and the heat input at the left end of the coil. The governing equation of the above problem is

$$-kA\frac{d^2t}{dx^2} + \beta\rho(T - T_\alpha) = 0, 0 < x < L \qquad (4)$$

We rewrite the above equation in the non-sinusoidal from

$$-\frac{d^2\theta}{dx^2} + m^2\theta = 0, 0 < x < L \qquad (5)$$

Where $\theta = (T - T_\alpha)$ being the temperature, and m^2 is given by

$$m^2 = \frac{\beta p}{Ak} = \frac{\beta\pi\rho}{\frac{1}{4}\pi D^2 k} = \frac{4\beta}{kD} \qquad (6)$$

The boundary condition of the problem becomes

$$\theta(0) = T(0) - T_\alpha = 500°\text{C}, \left(\frac{d\theta}{dx}\right)_{x=L} = 0 \qquad (7)$$

The boundary condition of the problem becomes

$$\theta(x) = \theta(0)\frac{\cosh m(L-x)}{\cosh mL}, Q(0) = \theta(0)\sqrt{\beta\rho Ak}\frac{\sinh mL}{\cosh mL} \qquad (8)$$

For the sake of comparison, both the finite difference and finite element solution of the problem are considered here.
i) Finite Difference solution:
The second derivative may be approximated with the centered finite difference expression in the following

$$\frac{d^2\theta}{dx^2} \approx \frac{1}{h^2}(\theta_{i+1} - 2\theta_i + \theta_{i-1}) \qquad (9)$$

Substituting the above formula for the second derivative into equation (5), we arrive at

$$-\theta_{i+1} + (2 + m^2h^2)\theta_i - \theta_{i-1} = 0 \qquad (10)$$

Which is valid for any point where θ is not specified.
At first a mesh of three points ($h = 0.0025$) is chosen, two end points and one in the middle. Applying the equation (10) at nodes 2 and 3, we obtain (m^2=400):

$$(2 + 400h^2)\theta_2 - \theta_3 = \theta_1, -\theta_2 + (2 + 400h^2)\theta_3 - \theta_4 = 0 \qquad (11)$$

Where $\theta_1 = \theta(0) = 500°$C.

It should be noted that θ_4 is the value of θ at the fictitious node 4, which is considered to be a mirror image because of the boundary condition of $d\theta/dx$.

To eliminate θ_4, one of the following expressions may be used:

$$\left(\frac{d\theta}{dx}\right)_{x=0} = \frac{\theta_4 - \theta5}{h} = 0 \text{ (forward)} \quad (12)$$

$$\left(\frac{d\theta}{dx}\right)_{x=0} = \frac{\theta_4 - \theta_2}{2h} = 0 \text{ (centered)} \quad (13)$$

The latter is of order $0(h^2)$, consistent with the centered difference equation no. (9). Using (13), $\theta_4 = \theta_2$ is set in equation 11. Equation (11) can be written in matrix form as

$$\begin{bmatrix} 2.25 & -1 \\ -2 & 2.25 \end{bmatrix} \left\{ \begin{array}{c} \theta_2 \\ \theta_3 \end{array} \right\} = \left\{ \begin{array}{c} 500 \\ 0 \end{array} \right\} \quad (14)$$

The solutions of these equations are

$$\theta_2 = 239.29°C, \theta_3 = 38.41°C \quad (15)$$

The heat at node $1(x = 0)$ can be computed using the definition

$$Q(0) = kA\left(-\frac{d\theta}{dx}\right)_{x=0} = kA\frac{\theta_1 - \theta_2}{h} = 5735.75 \text{ W} \quad (16)$$

Next, a mesh of five points is used. Applying equation (10) at nodes 2, 3, 4, 5 and using $\theta_6 = \theta_4$, we obtain ($h = 0.0125$)

$$\begin{vmatrix} 2.0625 & -1 & 0 & 0 \\ -1 & 2.0625 & -1 & 0 \\ 0 & -1 & 2.0625 & -1 \\ 0 & 0 & -2 & 2.0625 \end{vmatrix} \left\{ \begin{array}{c} \theta_2 \\ \theta_3 \\ \theta_4 \\ \theta_5 \end{array} \right\} = \left\{ \begin{array}{c} 500 \\ 0 \\ 0 \\ 0 \end{array} \right\} \quad (17)$$

$$\theta_2 = 336.61°C, \theta_3 = 194.27°C, \theta_4 = 64.06°C, \theta_5 = 62.12°C$$

The heat at node $1(x = 0)$ can be computed using the definition

$$Q(0) = kA\left(-\frac{d\theta}{dx}\right)_{x=0} = kA\frac{\theta_1 - \theta_2}{h} = 2463.92 \text{ W} \quad (18)$$

4. Relationship Between Virtual Reality Results and Real-World Experimentation

Fig. 9 shows the judgment between the measured emission levels for horizontal LLA's corresponding with LLAX and LLAY. Both of these represent the output of the EMI receiver with a line. The amplitude of the fundamental harmonic obtained by simulation [13] for the system configuration already described is represented with circles. It also signified the limit of the standard EN 55016-2-3 for high frequency series resonant inverters in domestic induction heater appliances. The LLAY can be seen to have a good arrangement with higher emission levels compared to LLAX. Here during measurements, some difficulties related to misalignment of the antennas were detected. Therefore some emissions assigned to the LLAY level measurement are presented in the LLAX signal.
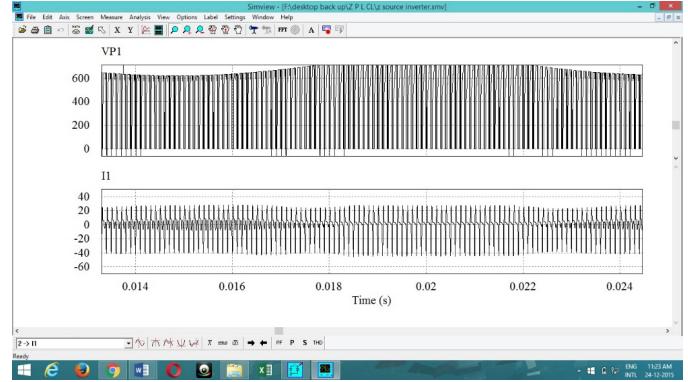

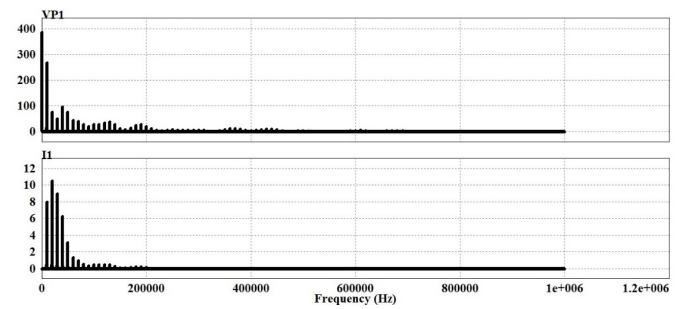Figure 9: Emission levels in the horizontal antennas in the induction heater

Figure 10: Emission levels in the vertical antenna LLAZ in the induction heater

Fig. 10 shows the emission levels associated with the vertical antenna LLAZ, which has an emission level permitted by the regulations which is higher than the one found in the horizontal antennas. Note that the agreement between the simulation results and the emission levels of the main harmonics is quite good for frequencies up to 55 MHz but, beyond this limit, major parasitic elements in the electrical system, not associated with the inductor, are needed to be considered to achieve accurate simulation results.

Interference by a high frequency series resonant inverter in a domestic induction heater used in emission control is required for high efficiency. Also it is required for heating non-ferromagnetic materials and eventually heat distribution in the cooking surfaces of the pan.

The inclusion of a high frequency resonant inverter for such applications is also essential for many other factors: design purpose, topology selection, calculation of design components, simulation of the designed system, prototype build up, prototype testing, EMI addition, design of the complete version and finally in testing the final version of the configuration.

At this point, the designer needs to determine the regulations governing the sale and use of the application.

5. Conclusion

This paper describes a procedure for obtaining emission levels of electromagnetic fields using computational methods in order to verify the compliance of the design with existing results obtained through laboratory measurements. This approach is very effective for high frequency series resonant inverters employed in domestic and industrial induction heaters. The process followed is verified by experimental measurements obtained in a precertification test under real conditions. The conformity achieved is quite satisfactory, allowing future improvements through simulation results, as the proposed method is also validated by experimental work.

References

[1] J. Acero, J. Burdio, L. Barragan, D. Navarro, R. Alonso, J. Garcia, F. Monterde, P. Hernandez, S. Llorente, I. Garde, The domestic induction heating appliance: An overview of recent research, in: 2008 Twenty-Third Annual IEEE Applied Power Electronics Conference and Exposition, 2008.

[2] C. Carretero, J. Acero, R. Alonso, J.M. Burdio, "Interference emission estimation of domestic induction cookers based on finite element simulation", Spanish MICINN under Project TEC2010-19207, Project CSD2009-00046, and Project IPT-2011-1158-920000, by the DGA-FSE, and by the Bosch and Siemens Home Appliances Group, 2011.

[3] A. M. Syaifudin, S. Mukhopadhyay, P. Yu, Electromagnetic field computation using comsol multiphysics to evaluate the performance of novel interdigital sensors, in: Applied Electromagnetics Conference (AEMC), 2009, IEEE, 2009, pp. 1–4.

[4] J. I. Artigas, I. Urriza, J. Acero, L. A. Barragan, D. Navarro, J. M. Burdio, Power measurement by output-current integration in series resonant inverters, IEEE Transactions on Industrial Electronics 56 (2) (2009) 559–567.

[5] D. Savia, Induction heating of samples in vacuum systems, in: The Proceeding of the COMSOL Users conference, 2007.

[6] D. Istardi, A. Triwinarko, Induction heating process design using comsol multiphysics software, TELKOMNIKA (Telecommunication Computing Electronics and Control) 9 (2) (2013) 327–334.

[7] M. Jungwirth, D. Hofinger, Multiphysics modelling of high-frequency inductive devices, in: The Proceeding of the COMSOL Users conference, 2007.

[8] A. Julegin, D. V., Coupled modelling of induction systems: heaters and power sources, HES-13 (2013) 237–243.

[9] D. Puyal, C. Bernal, J. Burdio, I. Millan, J. Acero, A new dynamic electrical model of domestic induction heating loads, in: Applied Power Electronics Conference and Exposition, 2008. APEC 2008. Twenty-Third Annual IEEE, IEEE, 2008, pp. 409–414.

[10] A. Boadi, Y. Tsuchida, T. Todaka, M. Enokizono, Designing of suitable construction of high-frequency induction heating coil by using finite-element method, IEEE Transactions on Magnetics 41 (10) (2005) 4048–4050.

[11] T. A. Jankowski, D. P. Johnson, J. D. Jurney, J. E. Freer, L. M. Dougherty, S. A. Stout, Experimental observation and numerical prediction of induction heating in a graphite test article, in: The Proceeding of the COMSOL conference, 2009.

[12] M. Fabbri, M. Forzan, S. Lupi, A. Morandi, P. L. Ribani, Experimental and numerical analysis of dc induction heating of aluminum billets, IEEE Transactions on Magnetics 45 (1) (2009) 192–200.

[13] J. Zgraja, J. Bereza, Computer simulation of induction heating system with series inverter, COMPEL-The international journal for computation and mathematics in electrical and electronic engineering 22 (1) (2003) 48–57.